Journal of ELECTRONIC MATERIALS, Vol. 38, No. 6, 2009
DOI: 10.1007/s11664-009-0728-0

Regular Issue Paper

Growth and Characterization of Zn-Incorporated Copper Oxide Films

M. ENGIN,[1] F. ATAY,[1,3] S. KOSE,[1] V. BILGIN,[2] and I. AKYUZ[1]

1.—Department of Physics, Eskisehir Osmangazi University, 26480 Eskisehir, Turkey.
2.—Department of Physics, Canakkale Onsekiz Mart University, 17100 Canakkale, Turkey.
3.—e-mail: fatay@ogu.edu.tr

In this work, undoped and Zn-doped copper oxide films were deposited on glass substrates at a substrate temperature of 250 ± 5°C by using an ultrasonic spray pyrolysis technique. Electrical, optical, and structural properties of the films were investigated, and the effect of Zn incorporation on these properties are presented. The variations of electrical conductivities and electrical conduction mechanisms of all films were investigated in the dark and in the light. Optical properties of the produced films were analyzed by transmission, linear absorption coefficient, and reflection spectra. The band gaps of the films were determined by an optical method. The film structures were studied by x-ray diffraction. To obtain information about structural properties in detail, the grain size (D), dislocation density (δ), and lattice parameters for preferential orientations were calculated. The elemental analyses were performed using energy-dispersive x-ray spectroscopy. It was concluded that Zn has a strong effect, especially on the electrical and structural properties, and the undoped and Zn-doped copper oxide (at 3%) films may be used as absorbing layers in solar cells due to their low resistivities and suitable linear absorption coefficient values.

Key words: Copper oxide films, ultrasonic spray pyrolysis, electrical and optical properties, XRD, EDS

INTRODUCTION

There are many well-known n-type transparent conductive oxide (TCO) materials such as ZnO, In_2O_3, and SnO_2. These materials are used as transparent electrodes in flat-panel displays, solar cells, and touch panels.[1] However, there are new TCOs with p-type conductivity such as copper oxide and copper aluminum oxide ($CuAlO_2$). Other p-type TCO thin films that are reported in the literature are $CuGaO_2$ and $SrCu_2O_2$. The development of p-type TCO materials is one of the key technologies for pn-junction-based oxide devices, such as diodes, transistors, and light-emitting diodes.[2,3] Copper oxide materials have unique features such as low cost and nontoxicity. Besides, copper is abundant, and the formation of the oxide layer is relatively simple. Additionally, a theoretical solar cell efficiency of 18% is predicted for such materials.[4] Copper oxide has two common forms: cupric oxide or tenorite (CuO) and cuprous oxide or cuprite (Cu_2O). CuO is a p-type semiconductor with a band gap of 1.9 eV to 2.1 eV and a monoclinic structure.[5,6] Cu_2O is also a p-type semiconductor with a band gap of 2.1 eV to 2.6 eV and a cubic structure.[5,7] It is known that duplex oxide films consisting of cupric oxide (CuO) as an outer layer and cuprous oxide (Cu_2O) as an inner layer are formed on copper during anodic oxidation in various electrolytes at room temperature as well as in air oxidation at elevated temperatures.[8] However, this binary system also contains other oxides such as Cu_3O_2 or Cu_4O_3 (paramelaconite).[9] Apart from their semiconductor applications, these materials have been employed as heterogeneous catalysts, solid-state gas sensors, heterocontacts,

(Received July 2, 2008; accepted February 10, 2009; published online March 5, 2009)

electrode materials for lithium batteries, and microwave dielectric materials.[10] Deposition of copper oxide thin films has been reported by various techniques, such as reactive magnetron sputtering,[6] reactive evaporation,[7] radiofrequency (RF) sputtering,[4] ion beam sputtering,[11] plasma evaporation,[12] sol–gel,[13,14] molecular beam epitaxy,[15] spin coating,[16] and solid-state reaction.[17] These studies reveal interesting size-dependent effects on the structural, optical, electrical, and magnetic behavior of nanocrystalline CuO.[18]

The aim of this work is to investigate the effect of Zn incorporation on the electrical, optical, and structural properties of copper oxide films produced by the ultrasonic spray pyrolysis (USP) technique and to research the availability capacities of the films for solar cell devices as absorbing layers.

EXPERIMENTAL DETAILS

Copper oxide and Zn-incorporated (at 1%, 3%, and 5%) copper oxide films were deposited onto glass substrates (objekttrager, 1 cm × 1 cm) by USP technique at a substrate temperature of 250 ± 5°C. Details of the USP technique were given in our previous works.[19,20] The spraying solution was prepared by dissolving $Cu(CH_3COO)_2 \cdot 2H_2O$ (0.1 M) and $Zn(CH_3COO)_2 \cdot 2H_2O$ (0.1 M) in distilled water. The solutions were mixed at certain volumes depending on the desired composition of the film. The volume of the starting spraying solution was 50 cc. The solution flow rate was controlled by a flowmeter and kept at 5 cc min^{-1}. Compressed purified air was used as the carrier gas (1 bar). The substrates were heated by an electrical heater, and the substrate temperature was measured using an iron-constantan thermocouple. The produced films were labeled BZ0, BZ1, BZ3, and BZ5, depending on the increasing Zn doping amount. The thickness of the films were measured using a metallurgical optical microscope. The codes and thicknesses of the copper oxide films are given in Table I. Current–voltage (*I–V*) measurements in the dark and in the light (10 mW/cm^2) were performed by using a Keithley 485 Autoranging Picaommeter and a Philip Harris 5 kV supply DC gauge. A tungstram incandescent lamp (300 W) was used as a light source, and light intensity was measured by using a 776 Solarmeter. Optical transmissions and absorptions of the films were recorded by a Perkin Elmer UV/VIS Lambda 2S spectrometer (double beam). The structures of the films were studied by an x-ray diffractometer (XRD) with CuK_α radiation (Rigaku model, λ = 1.5406 Å). The elemental analyses were made by energy-dispersive x-ray spectroscopy (EDS; Noran Voyager EDS 3050).

Table I. Codes and Thicknesses of the Copper Oxide Films

Material	Code	Thickness (μm)
Copper oxide	BZ0	0.53
Zn-incorporated copper oxide (at 1%)	BZ1	0.48
Zn-incorporated copper oxide (at 3%)	BZ3	0.38
Zn-incorporated copper oxide (at 5%)	BZ5	0.36

RESULTS AND DISCUSSION

Electrical Properties

Planar contacts were made through silver paste to determine the conduction mechanisms of the films. For all films, contact length and distance between two contacts were selected as ~1 mm and ~1.5 mm, respectively. The currents in the films were measured at room temperature in the dark and in the light (10 mW/cm^2) by applying voltage values between 12 V and 1000 V. The electrical conductivity type of BZ films was determined as *p*-type by using hot-probe technique.

Electrical Conduction Mechanisms

I–V characteristics of the films in the dark are shown in Fig. 1. It was clearly seen from Fig. 1 that the *I–V* variation of BZ3 films is linear, and the ohmic current mechanism is dominant. In the ohmic region, the number of free carriers is higher than the number injected into the semiconductor. Thus, the free carriers have more effect than the injected ones on the current. However, the whole voltage range was investigated in two regions for BZ0 and BZ5 films and in three regions for BZ1 films. In the first region (12 V to 40 V), current changes with voltage according to $I–V^{0.858}$ for BZ0, $I–V^{1.014}$ for BZ1, and $I–V^{0.995}$ for BZ5. So, ohmic conduction is dominant in the first region for three films. After the

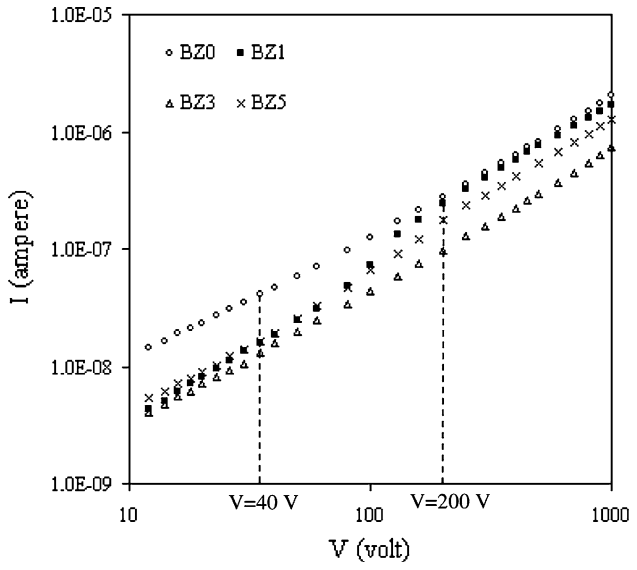

Fig. 1. *I–V* characteristics of BZ films in the dark.

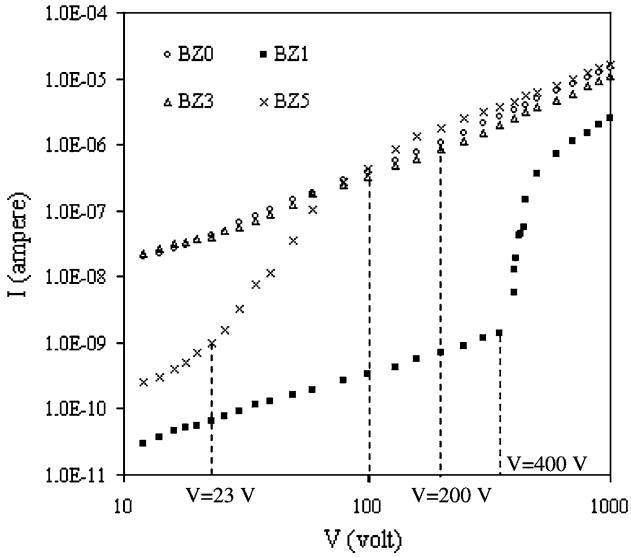

Fig. 2. *I–V* characteristics of BZ films in the light (10 mW/cm^2).

ohmic conduction region, the current change with voltage for BZ0 (40 V to 1000 V), BZ1 (40 V to 200 V), and BZ5 (40 V to 1000 V) films was of the form $I–V^{1.217}$, $I–V^{1.582}$, and $I–V^{1.421}$, respectively. These represent space-charge-limited (SCL) conduction regions where the traps start filling.[21] The transition voltage of the SCL region for the three films is V_{tr} = 40 V. In the SCL region, the charges are being trapped, and the number of injected carriers increases. Thus, both the free carriers and injected carriers contribute to the current. It was seen from Fig. 1 that BZ1 films have a third region (200 V to 1000 V) where the current changes with voltage according to $I–V^{1.167}$. In this region, the ohmic current mechanism is dominant. So, we think that the traps become ineffective above 200 V, and the contributions of the traps to the current start to decrease. After all investigations, it was determined that BZ0, BZ1, and BZ5 films have a shallow trapped structure in the dark.

I–V characteristics of the films in the light (10 mW/cm^2) are shown in Fig. 2. For BZ0 films, the current changed in the form $I–V^{1.273}$ in the 12 V to 200 V voltage range, and hence the SCL conduction mechanism is dominant. Beyond this region (200 V to 1000 V), the current change with voltage was of the form $I–V^{1.537}$. So, the SCL current mechanism is more dominant. This *I–V* behavior suggests that BZ0 films have a shallow trapped structure. It was seen from Fig. 2 that for BZ1 films the whole voltage range was investigated in three regions. Ohmic conduction is dominant in the first region between 12 V and 400 V ($I–V^{1.102}$), followed by a trap-filled-limited (TFL) conduction region. In the TFL region, all of the traps are almost filled, and the current increases sharply with increasing voltage. The transition from the ohmic region to the TFL region was observed at the voltage value of V_{TFL} = 400 V. BZ1 films have a third region where the current changes with voltage according to $I–V^{2.771}$. In this region, the current conforms to the trap-free square law, and the Fermi energy level nears the trap level. So, we can conclude that BZ1 films have a deep trapped structure. When the *I–V* characteristics of BZ3 films were investigated, it was determined that the current changed in the form $I–V^{0.732}$ and $I–V^{1.044}$ in the 12 V to 1000 V voltage range, and hence ohmic conduction mechanism is dominant. For BZ5 films, there are three regions. The first region indicates SCL current region where the current changed in the form $I–V^{2.230}$ in the 12 V to 23 V voltage range. The second region in the 23 V to 100 V voltage range is a TFL region where all of the traps are almost filled, and the transition voltage from the SCL region to TFL region is V_{TFL} = 23 V. In the third region (100 V to 1000 V), the current conforms to the trap-free square law ($I–V^{2.088}$).[21] So, it was determined that BZ5 films have a shallow trapped structure. However, for BZ5 films, an ohmic region was not observed because the current could not be measured in the 0 V to 12 V voltage range. The electrical conduction mechanisms of BZ films are listed in Table II. It is clearly seen that all films except for BZ3 have trapped structures.

Electrical Resistivities and Photoconductivities

Conductivities of the films were calculated by a two-probe technique in the dark and in the light (10 mW/cm^2). These calculations were made only using the current and voltage values in the ohmic regions since the films have trapped structures. The conductivities of all films are presented in Table III. It was seen that, in the dark condition, the conductivity of Zn-doped copper oxide films is almost the same as that of the undoped copper oxide films, but there is a slight decrease with Zn incorporation. The decrease in electrical conductivity of BZ0 films can be explained as follows: (i) the concentration of the free carriers in *p*-type BZ0 films decreases with

Table II. Electrical Conduction Mechanisms of BZ Films

Material	In Dark	In Light (10 mW/cm^2)
BZ0	Shallow trapped structure	Shallow trapped structure
BZ1	Shallow trapped structure	Deep trapped structure
BZ3	Ohmic current mechanism	Ohmic conduction mechanism
BZ5	Shallow trapped structure	Shallow trapped structure

Table III. Conductivity in Dark and Light Conditions, Photoconductivity, and Photosensitivity Values of BZ Films

Material	σ_d $(\Omega\ cm)^{-1}$	σ_l $(\Omega\ cm)^{-1}$	$\Delta\sigma = \sigma_l - \sigma_d$ $(\Omega\ cm)^{-1}$	$\Delta\sigma/\sigma_d$
BZ0	3.23×10^{-5}	5.68×10^{-5}	2.45×10^{-5}	0.76
BZ1	1.54×10^{-5}	1.26×10^{-7}	-1.53×10^{-5}	−0.99
BZ3	2.96×10^{-5}	8.06×10^{-5}	5.10×10^{-5}	1.72
BZ5	2.04×10^{-5}	–	–	–

Zn incorporation because Zn acts as a donor atom, i.e., while the free electron concentration in the conduction band increases with Zn incorporation, the free hole concentration in the valance band decreases to provide charge balance; (ii) scattering of the carriers at grain boundaries seems to be possible, because this scattering mechanism is responsible for the decrease of carrier mobility and hence the decrease of conductivity. Besides, it was determined from Table III that, in the light, the conductivity of BZ0 films decreased for 1% Zn incorporation and increased slightly for 3% Zn doping. When we compared the conductivities of the films in the dark with those in the light, it was seen that there is a slight increase in the conductivities of the BZ0 and BZ3 films and a clear decrease in the conductivities of the BZ1 films. This situation shows that light has a negative effect on BZ1 films. However, for BZ5 films, the conductivity values in the light were not calculated, because an ohmic region was not observed.

Photoconductivity ($\Delta\sigma = \sigma_l - \sigma_d$) and photosensitivity ($\Delta\sigma/\sigma_d$)[22] values were also calculated. There are three probable situations, as given below:

$$\Delta\sigma/\sigma_d < 0 \quad \text{for } \sigma_l < \sigma_d$$
(light reduces the conductivity)

$$\Delta\sigma/\sigma_d = 0 \quad \text{for } \sigma_l = \sigma_d \quad \text{(insensitive to light)}$$

$$\Delta\sigma/\sigma_d > 0 \quad \text{for } \sigma_l > \sigma_d$$
(light increases the conductivity).

The photoconductivity and photosensitivity values of the films are listed in Table III. As seen from the table, BZ0 and BZ3 films are photosensitive materials. For BZ1 films, the light has a reducing effect. We think that the free carrier concentration of BZ1 films increases due to the light. Thus, we concluded that the mobilities of the free carriers decrease since there are more free carriers in the structure. So, the decreasing conductivity can be explained by the diminishing mobility and various scattering mechanisms.

Optical Properties

Transmission spectra of BZ films are shown in Fig. 3. The transmittances of all films are high at long wavelengths, and the films behaved as transparent materials at about 800 nm to 1100 nm wavelength range. The transmittance values of the films decreased sharply below 800 nm because of their high absorbing properties. Also, all films behaved as opaque materials below 400 nm. It was seen that the optical transmittance values of BZ0 films were not changed noticeably by Zn incorporation. We think that this situation may be a result of the selected incorporation element, Zn. Since the atomic number of Zn is near to that of Cu, the number of valance electrons for Zn and Cu elements was not altered considerably.

Linear absorption coefficient ($\alpha = A/d$, where A is absorbance and d is thickness) spectra of BZ films are shown in Fig. 4. For $\lambda > 850$ nm, the absorption coefficient values of all films decrease weakly with increasing wavelength, and for $\lambda < 850$ nm they increase sharply with decreasing wavelength. However, for $\lambda < 850$ nm, there are two regions with a sharp increase in absorption values. We think that these regions are associated with the optical band gaps of BZ films. Besides, we concluded that the absorption coefficient spectra of the films are almost the same. This indicates that the fundamental absorption regions of BZ0 films were not changed remarkably by Zn incorporation. In other words, Zn incorporation does not have a strong effect on the absorption properties. However, the absorption coefficient values of BZ0 films were increased slightly with Zn incorporation of 3% and 5%.

Reflection (R) values of BZ films were calculated using the transmittance spectra and the equation given below,[23]

$$R = 1 - \sqrt{Te^{A}}. \qquad (1)$$

Reflection spectra of BZ films are shown in Fig. 5. It was clearly seen that the reflection values of the films are high, and there is not a noticeable change with Zn incorporation. This high value may be a result of the high free carrier concentration of all films. Besides, it was determined from the reflection spectra that the reflection values increased remarkably as the wavelength is reduced. At short wavelengths, as the energy of incident light increases, the interaction of light with electrons and the reflection properties of the films increase.

The transmission (T), reflection (R), and linear absorption coefficient (α) values of undoped and Zn-doped copper oxide films at 600 nm are given in Table IV. It was determined that Zn incorporation

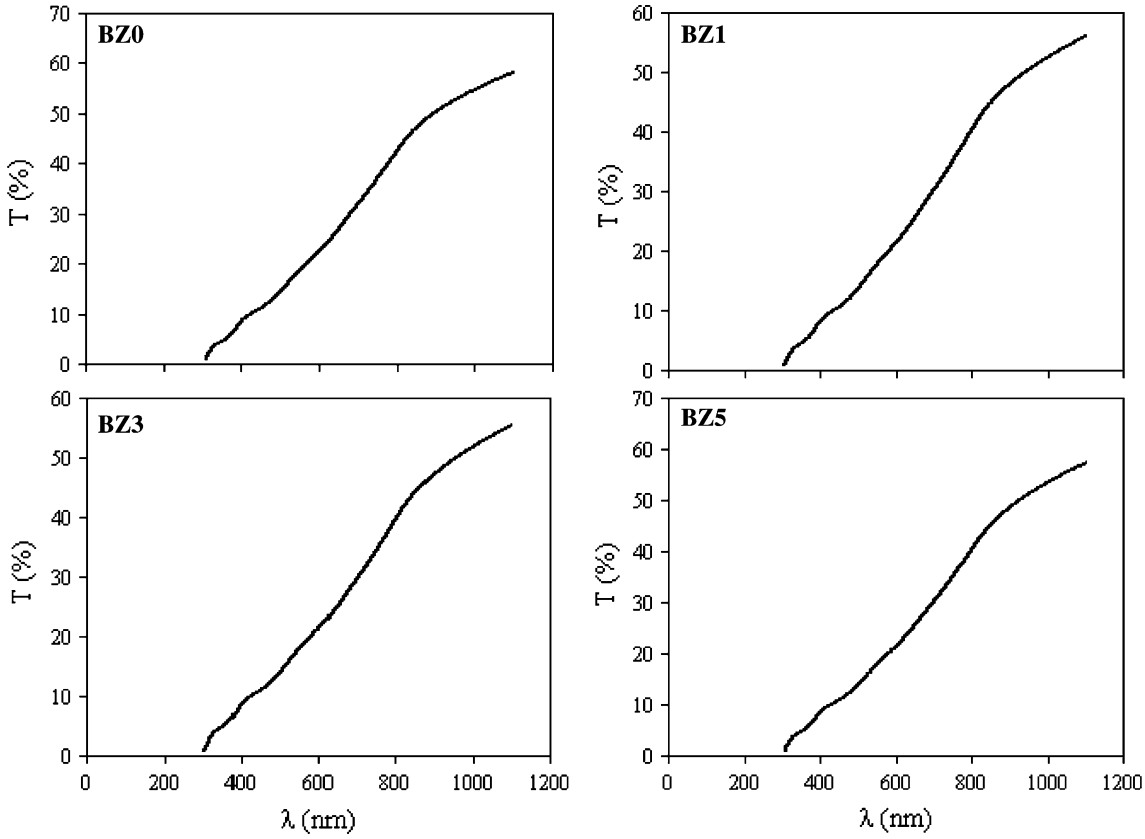

Fig. 3. Transmission spectra of BZ films.

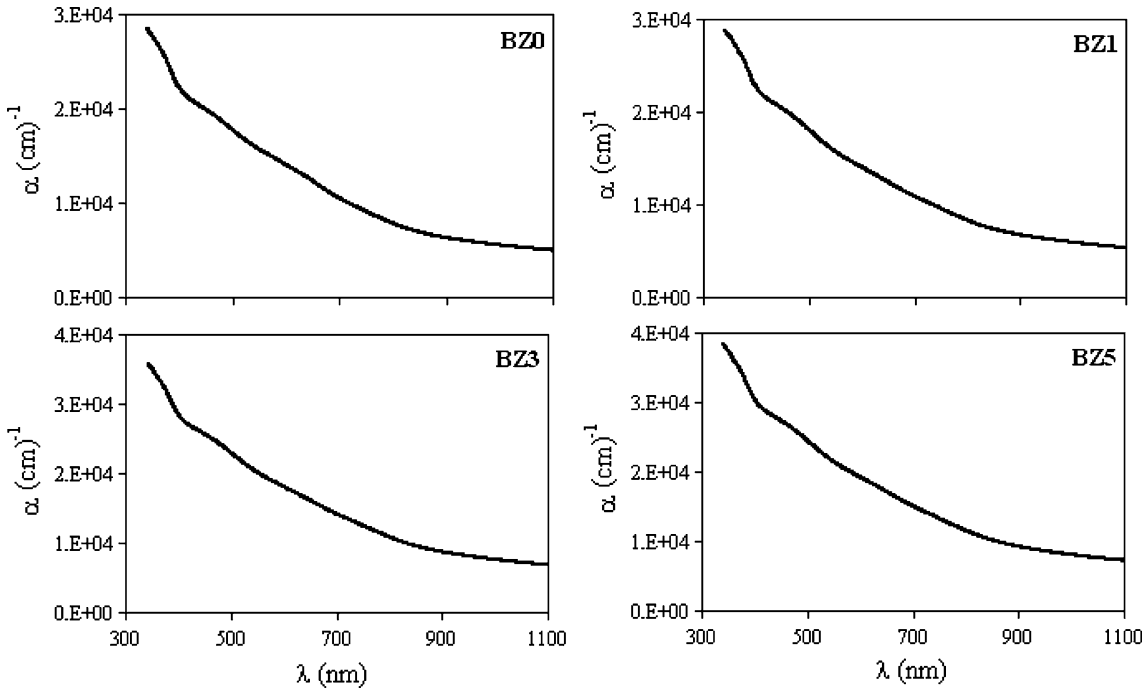

Fig. 4. Linear absorption coefficient spectra of BZ films.

has a weak effect on the optical properties of the films. Also, it was noted that the absorption properties of the films were improved with Zn incorporation of 3% and 5%. The absorption property of the films is a very important optical parameter because the copper oxide films are *p*-type materials. This

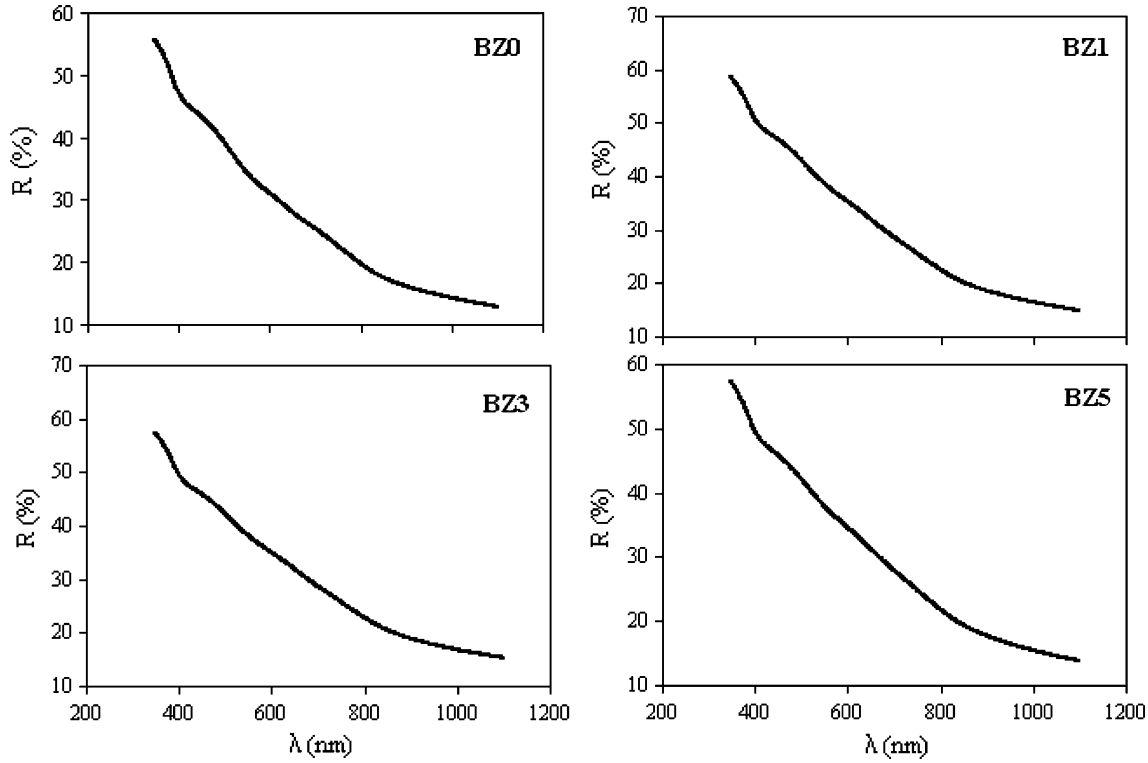

Fig. 5. Reflection spectra of BZ films.

Table IV. Transmission (T), Reflection (R), and Linear Absorption Coefficient (α) and the Optical Band Gap Values of BZ Films

λ = 600 nm	BZ0	BZ1	BZ3	BZ5
T (%)	22.54	21.34	21.27	21.42
R (%)	31.08	35.32	34.97	34.57
$\alpha \times 10^4$ (cm)$^{-1}$	1.41	1.40	1.81	1.92
E_{g1} (eV)	1.92	1.92	1.92	1.95
E_{g2} (eV)	2.64	2.65	2.64	2.64

shows that the absorption properties of copper oxide films containing higher Zn incorporations will be better.

Another important optical parameter is the band gap of materials that are used as absorbing layers in photovoltaic applications. The optical method was used to determine the band gaps of the prepared undoped and Zn-doped copper oxide films in this work. The band gap values were obtained by extrapolating the linear portion of plots of $(\alpha h\nu)^2$ versus $h\nu$ to $(\alpha h\nu)^2 = 0$. These plots of BZ films are given in Fig. 6. First of all, from the plots it was determined that all films have direct band gaps. This property is suitable for photovoltaic solar cells. Secondly, there are two linear regions with different slopes for all films. Using these slopes, two different energy gap values were calculated as E_{g1} and E_{g2}. Here, E_{g1} refers to the band gaps of CuO, while E_{g2} represents those of Cu_2O. The values are listed in Table IV. It is seen from this table that the E_{g1} values of the films were found to be between 1.92 eV and 1.95 eV, and the E_{g2} values of the films were found to be between 2.64 eV and 2.65 eV. These values are in good agreement with the literature.[5–7] Besides, it was determined from Table IV that Zn incorporation does not have a strong effect on the band gaps of the undoped films due to the low Zn incorporation fractions selected in this work.

Structural Properties

XRD patterns of BZ films are shown in Fig. 7. It was determined that all films have a polycrystalline structure since these patterns include peaks with different intensities and half-widths. Harris analysis was performed to determine the preferential orientations. The texture coefficient was calculated using the equation below[24,25]:

$$P(h_i k_i l_i) = \frac{I(h_i k_i l_i)}{I_0(h_i k_i l_i)} \left[\frac{1}{n} \sum_{i=1}^{n} \frac{I(h_i k_i l_i)}{I_0(h_i k_i l_i)} \right]^{-1}, \quad (2)$$

where I_0 represents the standard intensity (American Society of Testing Materials, ASTM), I is the measured intensity of the $(h_i k_i l_i)$ plane and n is the reflection number. $P(h_i k_i l_i)$ has to be larger than unity to determine the preferential orientation.[26] The angle of diffraction (2θ), lattice spacing (d), Miller indices (hkl), crystal system, relative

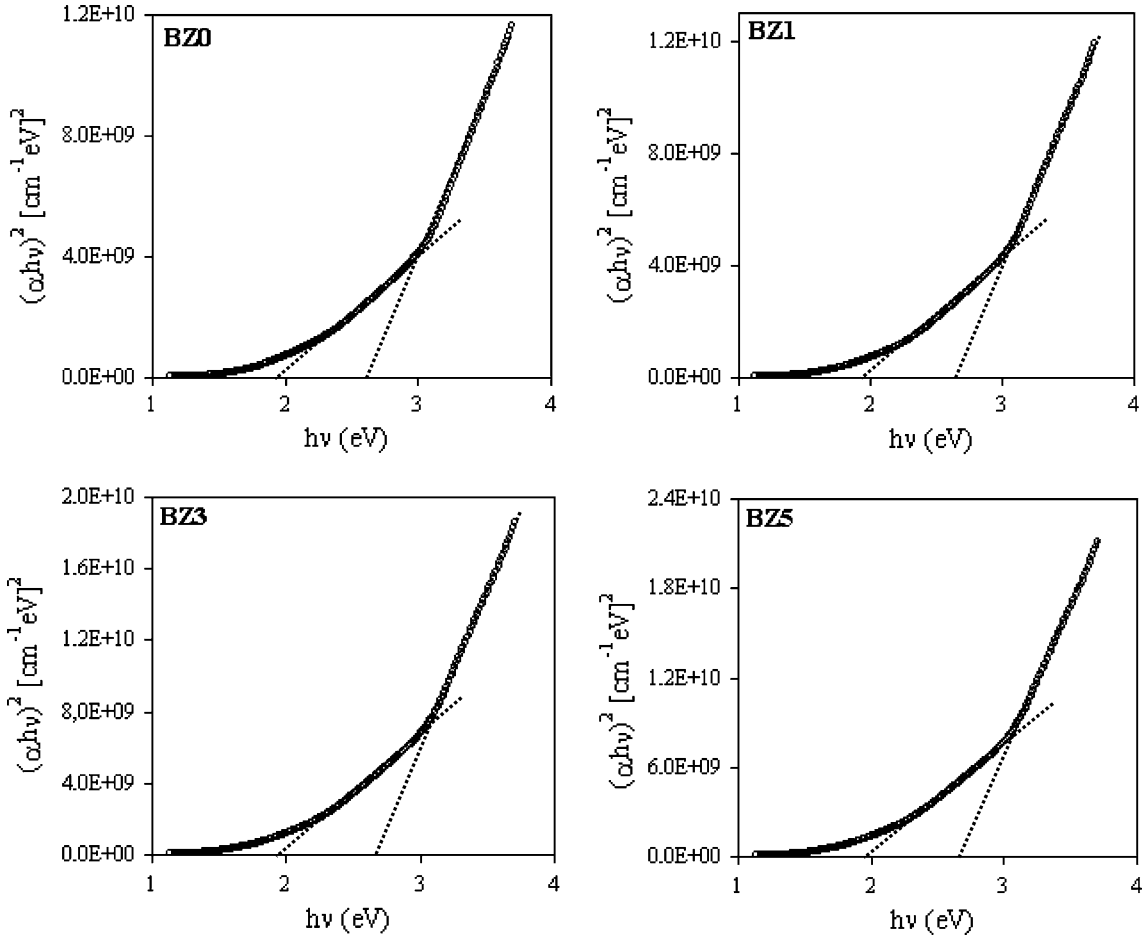

Fig. 6. Plots of $(\alpha h\nu)^2$ versus $h\nu$ of BZ films.

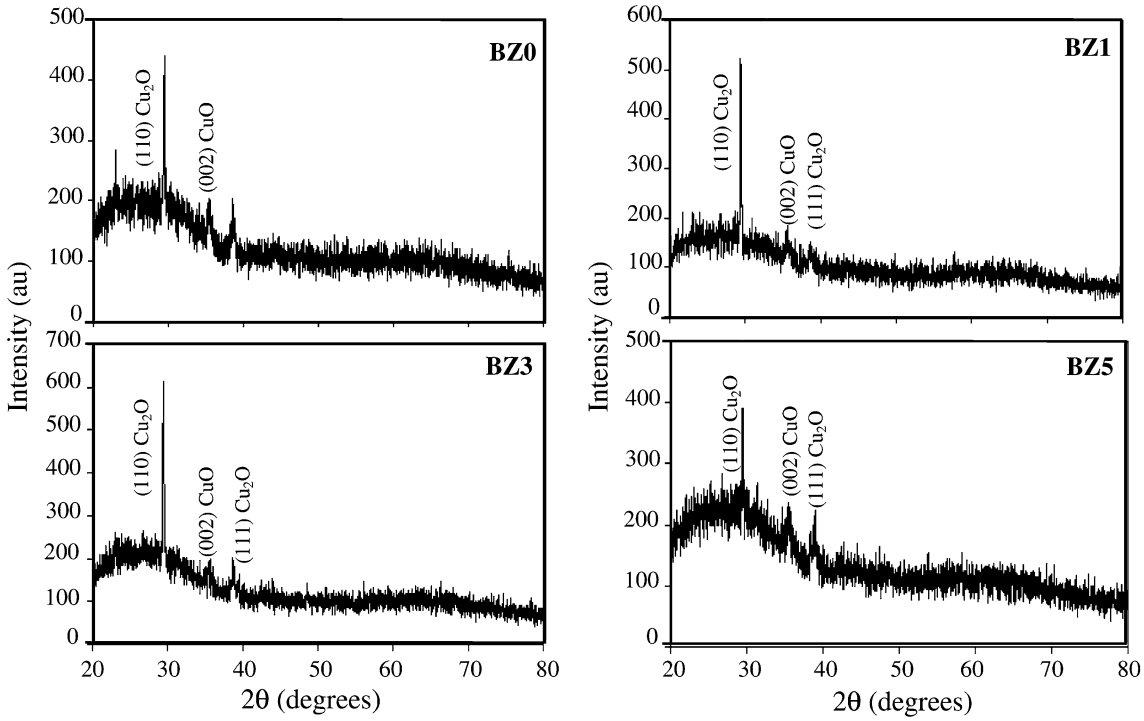

Fig. 7. XRD patterns of BZ films.

intensity (I/I_0), and texture coefficient (P) are listed in Table V. It is seen from Table V that BZ films consisted of two phases, Cu_2O (cuprite) and CuO (tenorite). When the calculated texture coefficient values for the three peaks given in Table V were investigated, it was determined that the texture coefficient values of the peaks at 2θ = 29.40 deg, 29.63 deg, 29.53 deg, and 29.38 deg are larger than those for BZ0, BZ1, BZ3, and BZ5 films, respectively. So, it was concluded that the preferential orientation of all BZ films is the (110) direction, and the Cu_2O phase is more dominant than the CuO phase. Besides, it was seen from Fig. 7 that the intensity of the (110) peak for BZ1 and BZ3 films was increased slightly as compared with BZ0. So, we can say that Zn incorporation at 1% and 3% improved the structure. Furthermore, BZ1 and BZ3 films have a more stable phase because unstable CuO phases became recessive with Zn incorporation at 1% and 3%. However, as compared with the XRD patterns of BZ5 films, it was determined that especially the intensity of the (110) peak was decreased, and the intensities of the (002) and (111) peaks were increased. This situation indicated that the unstable CuO phases became dominant again with Zn incorporation at 5%. It was concluded that the crystallinity levels of the undoped copper oxide films improved with Zn incorporation at 1% and 3% because of the recessive unstable CuO phases and deteriorated with Zn doping at 5% on account of the dominant unstable CuO phases. So, we think that Zn incorporation at 5% is not a suitable doping ratio, especially in terms of structural properties.

To obtain information about structural properties in detail, the grain size (D) using Scherrer formula, dislocation density (δ), and lattice parameters ($a = b = c$ for cubic structure) for preferential orientations were calculated using the formulas given below[27,28]:

$$D = \frac{0.9\lambda}{B\cos\theta}, \tag{3}$$

$$\delta = \frac{1}{D^2}, \tag{4}$$

$$d_{hkl} = \left[\frac{1}{a^2}(h^2 + k^2 + l^2)\right]^{-1/2}, \tag{5}$$

where B is the half-width in radians of the peak with maximum intensity, D is the grain size, θ is the Bragg angle, and λ is the wavelength of the light used. The dislocation density (δ) is defined as the length of dislocation lines per unit volume of the crystal. Higher δ values indicate lower crystalline levels for the films since these values indicate the amount of defects in the structure. Structural parameters such as the full-width at half-maximum (FWHM, B), grain size, and dislocation density values for all films are given in Table VI. It is clearly seen that the B and δ values decreased, while D values increased with Zn incorporation. The increase of grain size, especially with Zn incorporation at 1% and 3%, highlights the decrease of the grain boundaries, and thus the crystallinity level of undoped copper oxide films improves with Zn doping at 1% and 3%. In addition, BZ1 and BZ3 films have lower δ values. This situation also indicates that these films have higher crystalline levels because of the decreased dislocation defects in the film. According to these results, we can verify that the structural properties of the undoped copper oxide films are improved with Zn incorporation at 1% and 3%. Also, it was determined that BZ3 films have the lowest dislocation density and the highest grain size values. So, it is concluded that Zn incorporation at 3% has a desired effect on the structural properties. The calculated values and ASTM values of the lattice parameters and the volume of unit cell for the preferential orientations are given in Table VI. It is seen that the values are in good agreement with each other.

EDS analyses of the samples deposited at different Zn concentrations were taken in order to see

Table V. Angle (2θ), Lattice Spacing (d), Miller Indices (hkl), Crystal System, Relative Intensity (I/I_0), and Texture Coefficient (P) of BZ Films

Material	2θ (deg)	d (Å)	(hkl)	Crystal System	I/I_0 (%)	P
BZ0	29.40	3.036	(110)	Cu_2O	100	3.39
	35.40	2.533	(002)	CuO	24	0.15
	38.30	2.348	(111)	CuO	24	0.11
BZ1	29.63	3.013	(110)	Cu_2O	100	2.82
	35.36	2.537	(002)	CuO	14.1	0.49
	38.52	2.335	(111)	CuO	12.9	0.19
BZ3	29.53	3.023	(110)	Cu_2O	100	3.37
	35.43	2.532	(002)	CuO	12.3	0.28
	38.76	2.321	(111)	CuO	14.7	0.10
BZ5	29.38	3.038	(110)	Cu_20	100	3.03
	35.55	2.523	(002)	CuO	37.4	0.44
	38.76	2.321	(111)	CuO	31.3	0.15

Table VI. Full-Width at Half-Maximum (FWHM, *B*), Grain Size (*D*), Dislocation Density (δ), and Calculated Values and ASTM Values of Lattice Parameters and Volume of Unit Cell for Preferential Orientations for BZ Films

Preferential Orientation (110)	BZ0	BZ1	BZ3	BZ5
$B \times 10^{-3}$ (Radian)	3.35	2.29	2.58	3.05
D (Å)	428	514	555	470
$\delta \times 10^{-6}$ (Å)$^{-2}$	5.46	3.78	3.25	4.52
Calculated ($a = b = c$) (Å)	4.29	4.26	4.28	4.30
ASTM ($a = b = c$) (Å)	4.27	4.27	4.27	4.27
Calculated V (Å)^3	79.2	77.4	78.1	79.3
ASTM V (Å)^3	77.8	77.8	77.8	77.8

Table VII. EDS Results of BZ Films

	BZ0		BZ1		BZ3		BZ5	
Element	**wt.%**	**at.%**	**wt.%**	**at.%**	**wt.%**	**at.%**	**wt.%**	**at.%**
Na-K	6	7	4	4	–	–	5	5
Mg-K	1	1	1	1	1	1	1	1
Si-K	24	21	24	21	30	26	25	22
Ca-K	4	2	4	3	5	3	4	2
Cu-L	26	10	23	9	7	3	21	8
O	38	59	38	59	43	63	39	59
Zn-L	–	–	5	2	13	5	5	2

whether Cu, O, and Zn elements in the starting solutions were present in the solid films or not. The EDS results of BZ films are listed in Table VII, which shows that the expected elements exist in the solid films, and Zn was really doped in the films. Na, Mg, Si, and Ca elements are also present in the solid films. It is thought that these elements may probably result from the glass used as the substrate.

CONCLUSIONS

In this work, the effect of Zn incorporation on electrical, optical, and structural properties of *p*-type copper oxide films were investigated, and the available capacities of the films as absorbing layers for solar cell devices were investigated. To produce the films a USP technique was used since the cost of the produced material is a very important criterion for solar cells. The electrical investigations showed that BZ0, BZ1, and BZ5 films have a shallow trapped structure, and the ohmic current mechanism is dominant for BZ3 films in the dark. In the light (10 mW/cm^2), it was determined that all films except BZ3 have trapped structures. Also, the conductivities of the films were calculated in the dark and in the light. It was seen that, in the dark, there is a slight decrease with Zn incorporation. We think that this decrease can result from the decreasing free charge carriers of *p*-type BZ0 films with Zn incorporation and/or scattering of carriers at grain boundaries. Besides, it was determined that BZ0 and BZ3 films are photosensitive materials. The optical investigations give us the following important information: (i) The linear absorption coefficient values are suitable for absorbing layers in photovoltaic applications, and the absorption properties of BZ films were improved by Zn incorporation of 3% and 5%. (ii) All films have direct band structures and two different band gap values, related to CuO and Cu_2O phases. From the structural analyses, it was determined that all films have a polycrystalline structure. It was concluded that the preferential orientation of all films is the (110) direction, and the Cu_2O phase is more dominant than the CuO phase. It was determined that the crystallinity of the BZ0 films improved with Zn incorporation at 1% and 3% on account of the recessive unstable CuO phases, and deteriorated with Zn doping at 5% on account of the dominant unstable CuO phases. It was determined that BZ3 films have the lowest dislocation density and the highest grain size values. So, it is concluded that Zn incorporation at 3% has a positive effect on structural properties. It was determined from EDS analyses that Zn has really been incorporated. Consequently, we can say that Zn has a strong effect, especially on the electrical and structural properties. Besides, we concluded that undoped and Zn-doped copper oxide (at 3%) films may be used as absorbing layers for solar cells due to their low resistivities and suitable linear absorption coefficient values. We believe that, by trying different

experimental parameters such as substrate temperature, flow rate, and incorporation amount in our future work, films with only stable CuO phases can be produced by USP technique to obtain higher efficiencies in solar cell devices. CuO films are more suitable candidates for absorbing layers due to their lower optical band gaps.

REFERENCES

1. H. Yanagi, S. Inoue, K. Ueda, H. Kawazoe, H. Hosono, and N. Hamada, *J. Appl. Phys.* 88, 4159 (2000). doi:10.1063/1.1308103.
2. K. Tonooka, K. Shimokowa, and O. Nishimura, *Thin Solid Films* 411, 129 (2002). doi:10.1016/S0040-6090(02)00201-8.
3. A.N. Banerjee, S. Kundoo, and K.K. Chattopadhyay, *Thin Solid Films* 440, 5 (2003). doi:10.1016/S0040-6090(03)00817-4.
4. S. Ghosh, D.K. Avasthi, P. Shah, V. Ganesan, A. Gupta, D. Sarangi, R. Bhattacharya, and W. Assmann, *Vacuum* 57, 377 (2000). doi:10.1016/S0042-207X(00)00151-2.
5. S.C. Ray, *Sol. Energy Mater. Sol. Cells* 68, 307 (2001). doi:10.1016/S0927-0248(00)00364-0.
6. J.F. Pierson, A. Thobor-Keck, and A. Billard, *Appl. Surf. Sci.* 210, 359 (2003). doi:10.1016/S0169-4332(03)00108-9.
7. B. Balamurugan and B.R. Mehta, *Thin Solid Films* 396, 90 (2001). doi:10.1016/S0040-6090(01)01216-0.
8. M. Seo, Y. Ishikawa, M. Kodaira, A. Sugimoto, S. Nakayama, M. Watanabe, S. Furuya, R. Minamitani, Y. Miyata, A. Nishikata, and T. Notoya, *Corros. Sci.* 47, 2079 (2005). doi:10.1016/j.corsci.2004.09.016.
9. A. Thobor and J.F. Pierson, *Mater. Lett.* 57, 3676 (2003). doi:10.1016/S0167-577X(03)00148-4.
10. J. Morales, L. Sanchez, F. Martin, J.R. Ramos-Barrado, and M. Sanchez, *Thin Solid Films* 474, 133 (2005). doi:10.1016/j.tsf.2004.08.071.
11. K.H. Yoon, W.J. Choi, and D.H. Kang, *Thin Solid Films* 372, 250 (2000). doi:10.1016/S0040-6090(00)01058-0.
12. K. Santra, C.K. Sarker, M.K. Mukherjee, and B. Ghosh, *Thin Solid Films* 213, 226 (1992). doi:10.1016/0040-6090(92)90286-K.
13. M.T.S. Nair, L. Guerrero, O.L. Arenas, and P.K. Nair, *Appl. Surf. Sci.* 150, 143 (1999). doi:10.1016/S0169-4332(99)00239-1.
14. A.Y. Oral, E. Mensur, M.H. Aslan, and E. Basaran, *Mater. Chem. Phys.* 83, 140 (2004). doi:10.1016/j.matchemphys.2003.09.015.
15. K.P. Muthe, J.C. Vyas, S.N. Narang, D.K. Aswal, S.K. Gupta, D. Bhattacharya, R. Pinto, G.P. Kothiyal, and S.C. Sabharwal, *Thin Solid Films* 324, 37 (1998). doi:10.1016/S0040-6090(97)01203-0.
16. M.A. Brookshier, C.C. Chusuei, and D.W. Goodman, *Langmuir* 15, 2043 (1999). doi:10.1021/la981325k.
17. J.F. Xu, W. Ji, Z.X. Shen, S.H. Tang, X.R. Ye, D.Z. Jia, and X.Q. Xin, *Solid State Chem.* 147, 516 (1999). doi:10.1006/jssc.1999.8409.
18. M. Parhizkar, S. Singh, P.K. Nayak, N. Kumar, K.P. Muthe, S.K. Gupta, R.S. Srinivasa, S.S. Talwar, and S.S. Major, *Colloids Surf. A: Physicochem. Eng. Aspects* 257–258, 277 (2005). doi:10.1016/j.colsurfa.2004.10.029.
19. F. Atay, V. Bilgin, I. Akyuz, and S. Kose, *Mater. Sci. Semicond. Process.* 6, 197 (2003). doi:10.1016/S1369-8001(03)00085-4.
20. F. Atay, S. Kose, V. Bilgin, and I. Akyuz, *Mater. Lett.* 57, 3461 (2003). doi:10.1016/S0167-577X(03)00100-9.
21. M.A. Lampert and P. Mark, *Current Injection in Solids* (NY: Academic, 1970), p. 347.
22. S. Brushan and S.K. Sharma, *J. Mater. Sci.: Mater. Electron.* 1, 165 (1990). doi:10.1007/BF00694738.
23. M.E. Ozsan, D.R. Johnson, M. Sadeghi, D. Sıvapathasundaram, G. Goodlet, M.J. Furlong, L.M. Peter, and A.A. Shingleton, *J. Mater. Sci.: Mater. Electron.* 7, 119 (1996). doi:10.1007/BF00225634.
24. C.S. Barrett and T.B. Massalski, *Structure of Metals* (Oxford: Pergamon, 1980), p. 204.
25. V. Bilgin, S. Kose, F. Atay, and I. Akyuz, *J. Mater. Sci.* 40, 1909 (2005). doi:10.1007/s10853-005-1210-x.
26. J.P. Nair, R. Jayakrishnan, N.B. Chaure, and R.K. Pandey, *Semicond. Sci. Technol.* 13, 340 (1998). doi:10.1088/0268-1242/13/3/002.
27. R. Mamazza Jr, D.L. Morel, and C.S. Ferekides, *Thin Solid Films* 484, 26 (2005). doi:10.1016/j.tsf.2005.01.097.
28. R. Ferro, J.A. Rodriguez, O. Vigil, and A. Morales-Acevedo, *Mater. Sci. Eng. B* 87, 83 (2001). doi:10.1016/S0921-5107(01)00620-1.